

Comparing different solutions for testing resistive defects in low-power SRAMs

*Original*

Comparing different solutions for testing resistive defects in low-power SRAMs / Mirabella, Nunzio; Grosso, Michelangelo; Franchino, Giovanna; Rinaudo, Salvatore; Deretzis, Ioannis; La Magna, Antonino; Sonza Reorda, Matteo. - ELETTRONICO. - (2021), pp. 1-6. ( 22nd IEEE Latin-American Test Symposium 2021 Porto Alegre (Brazil) 27th - 29th October 2021) [10.1109/lats53581.2021.9651760].

*Availability:*

This version is available at: 11583/2920394 since: 2022-04-06T13:27:14Z

*Publisher:*

Institute of Electrical and Electronics Engineers Inc.

*Published*

DOI:10.1109/lats53581.2021.9651760

*Terms of use:*

This article is made available under terms and conditions as specified in the corresponding bibliographic description in the repository

*Publisher copyright*

IEEE postprint/Author's Accepted Manuscript

©2021 IEEE. Personal use of this material is permitted. Permission from IEEE must be obtained for all other uses, in any current or future media, including reprinting/republishing this material for advertising or promotional purposes, creating new collecting works, for resale or lists, or reuse of any copyrighted component of this work in other works.

(Article begins on next page)

DX.DOI.ORG/10.19199/2021.2-3.1121-9041.05

## Characterization of marble weathering through pore structure quantitative analysis

Stone weathering is strongly controlled by the intrinsic properties of the stone and by its use. Previous studies demonstrate that the response to natural or artificial ageing processes of the rocks seems to be strongly influenced by the pore structure of the stone. A better understanding of this phenomenon is provided by the study and characterization of porosity and of the pore structure at different degrees of alteration. The analysis of the evolution of the decay leads to the evaluation of the durability of marble in facades, and more generally in buildings, as well as for the protection and recovery of artistic and architectural heritage.

In this paper, we apply a methodology for the geometrical characterization of the pore structure to quantify alteration induced by natural weathering on marble slabs. The approach is based on the application of a path-finding algorithm to 2D binary images representative of thin sections of marble at different degrees of alteration. Through the identification of the paths within the porous domain, the methodology allows the characterization of the pore structure in terms of pore radius distribution along the identified paths. Analysis of the results demonstrate a good agreement between the degree of alteration of the pore structure and the corresponding variation of the physical and mechanical properties of the rock samples under investigation.

**Keywords:** marble, weathering, microscope images, pore radius, path-finding algorithm, pore structure characterization.

**Caratterizzazione dell'alterazione del marmo dovuta ad agenti atmosferici mediante analisi quantitativa della struttura porosa.** L'invecchiamento delle pietre ornamentali è fortemente condizionato dalle proprietà intrinseche della pietra e dal contesto di utilizzo. Precedenti studi dimostrano che la risposta ai processi di invecchiamento naturale o artificiale delle rocce è influenzata dalla struttura dei pori della pietra stessa. Questo fenomeno può essere meglio compreso attraverso lo studio e la caratterizzazione della porosità e della struttura dei pori a diverso grado di alterazione. Informazioni utili sull'evoluzione del degrado portano alla valutazione della durabilità del marmo nelle facciate, e in generale negli edifici, e alla tutela e il recupero del patrimonio artistico e architettonico.

In questo articolo, applichiamo un approccio per la caratterizzazione geometrica dei parametri della struttura dei pori per quantificare l'alterazione naturale indotta dagli agenti atmosferici su lastre di marmo. La metodologia si basa sull'applicazione di un algoritmo di ricerca del percorso ad immagini binarie 2D rappresentative di sezioni sottili del marmo a diversi livelli di alterazione.

I risultati forniti dai test preliminari confermano una buona concordanza tra la struttura dei pori e la corrispondente variazione delle proprietà fisiche e meccaniche del campione analizzato.

**Parole chiave:** marmo, agenti atmosferici, immagini al microscopio, raggio dei pori, algoritmo di path-finding, caratterizzazione della struttura porosa.

### 1. Introduction

Stone weathering is controlled by the intrinsic properties of the stone (mineralogical-petrographic, porosity and mechanical features)

and by its uses (external and internal facades, paving, roofs etc.).

Previous studies underlined the influence of porosity in the weathering evolution processes in natural stones (Hudec, 1998;

Costanzo Peter\*\*  
 Oliviero Baietto\*  
 Rossana Bellopede\*  
 Filippo Panini\*  
 Eloisa Salina Borello\*\*  
 Paola Marini\*  
 Dario Viberti\*

\* Politecnico di Torino, Turin, Italy

\*\* Center for Sustainable Future Technologies, Fondazione Istituto Italiano di Tecnologia, Turin, Italy

Corresponding author: Costanzo Peter  
 costanzo.peter@polito.it

Siegesmund, 2008; Molina Ballesteros *et al.*, 2010) even in marble, characterized by a low porosity (Siegesmund, 2000, Sassoni *et al.*, 2014). Many tests of artificial and natural ageing, together with in situ analysis on exposed marbles, showed that an increase in weathering is connected to an increase in porosity as well as to a decrease in mechanical resistance (Warke *et al.*, 2006; Bellopede *et al.*, 2016).

The response to natural or artificial ageing processes seems to be strongly influenced by the pore structure of the stone. The presence of closed or interconnected voids in compact rock is one of the main features that needs thorough investigation.

Due to the existing correlation between movement of the fluids, such as water, and weathering, the analysis of the porosity evolution within a rock is the most interesting approach in order to investigate the correlation between decay and structure.

The study of the increase of total porosity and of the geometrical characteristic of the pore structure provides useful information on the evolution of the decay, and it allows evaluating the marble durability in facades, and more generally in buildings, as well as for the

protection and recovery of artistic and architectural heritage.

In this paper, we apply a methodology recently presented by Viberi *et al.* 2020 for the geometrical characterization of the pore structure parameters to quantify marble weathering.

Porous media are complex materials characterized by a chaotic structure and tortuous fluid flow, with pore and grains dimension varying over a wide range (Ghanbarian *et al.* 2013). Pore network model is considered to be an important platform for describing the geometry and topology of pore spaces and for performing flow calculations (Yao *et al.* 2015). Characterization of porous media geometry and properties, at different scales, is fundamental for several fields of application and scientific disciplines such as geology, reservoir engineering, underground water science, chemistry, material science and engineering.

The study of the pore characteristics has an important historical background, starting from ancient Egyptians, Greeks and Romans, passing through the significant progress in scientific evaluation during 19<sup>th</sup> century with the introduction of physical principles such as capillarity, diffusion and fluid flow, leading up to the modern experimental methodologies (Sing, 2004). In the last decades, the adoption of addressed experimental procedures coupled with the possibility to acquire high resolution images of porous media (microscope, etc.), several approaches for 2D pore structure image analysis have been developed and presented in the technical literature. These include grain recognition (Oren & Bakke, 2003), medial-axis (Lindquist *et al.*, 1996), medial surface (Al-Raoush and Madhoun, 2017), fractal geometry (Xu *et al.*, 2008; Xiao *et al.*, 2019; Cai *et al.*, 2019), Dijkstra's algorithm (Sun *et al.*, 2011), watershed (Sheppard

*et al.*, 2004; Rabbani, *et al.* 2014) and percolation theory (Liu *et al.*, 2014).

In this paper we present a methodological approach for the investigation of the effect of weathering on marble samples through the application of a modified version of the A\* path-finding algorithm. The pore structure characterization is carried out on macroscope-acquired images of marble thin sections at different degrees of alteration. The acquired images are then binarized so as to identify the porous domain within which the paths are calculated by A\*. The visible paths can be exploited for pore structure characterization: along each path, the aperture of the channels can be estimated. An example of application of the methodology and the analysis of the output results is presented.

## 2. Dataset description and experimental procedure

### 2.1. Rock sample description

The methodology was applied to a case study of a Marble identified as ITQ4 quarried in Stazzena (LU).

The hand sample is a compact white breccia, characterized by veins varying in color from brown

to dark gray with a very variable pattern and size. The marble clasts are elongated and stretched, with pluridecimeteric dimensions, immersed in a locally dark gray cement.

The thin section shows a crystalloblastic metamorphic lithotype. Anisotropic blasts with mainly interlobate, inequigranular edges (300 ÷ 350 µm) are present in the clasts which are surrounded by an inequigranular calcitic mosaic of subhedral blasts with rounded and rectilinear edges (100 µm). Complex veins consisting of pyrite, quartz, sericite, muscovite, epidote, titanite and opaque are present (Fig. 1).

### 2.2. Weathering

Stone weathering is correlated with many different physicochemical processes (Bortz *et al.*, 1993, Winkler, 1987) operating both sequentially and synergistically (Bellopede *et al.*, 2016). Previous studies (e.g. Camuffo, 1995) proved that the aesthetic value loss is directly related to the intrinsic properties of the material as well as to natural agents. Rainwater, wind, solar radiation and thermic variations are the primary causes for the mechanical and physical weakening of stones. Moisture, which affects the inter-particle forces acting on independent granules,

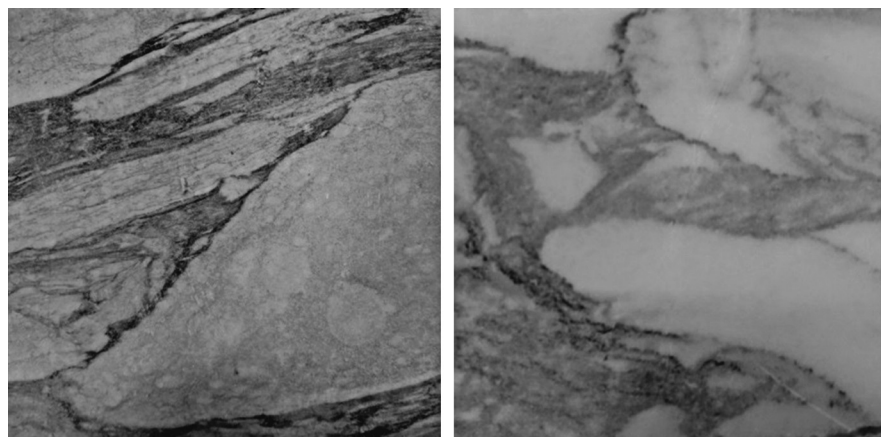


Fig. 1 – Comparison between non altered ITQ4 sample (left) and weathered slab (right).

is a critical factor for weathering processes, and the water movement within the bulk volume of the stone is strongly related to the porosity and the permeability of the material (Warke *et al.*, 2006). Moreover, the natural decay deeply modifies the edges between grains, it widens cracks resulting in an increase in porosity.

This indicates that the variation of the pore characteristics, such as open porosity, pore size and shape, depends on the weathering trend. These characteristics are important variables that may change with time, especially in the subsurface layer where the main physical, chemical and biological processes occur (Biscontin *et al.*, 1993).

The two analyzed samples come from two 50 x 70 cm slabs of ITQ4 marble. One underwent natural weathering, through ten years of outdoor exposure, while the second is the original sample that was kept indoors.

From the two original samples, the specimens have been cut and several thin sections were obtained from both the weathered and the original slab. The thin sections were impregnated with a blue methylene liquid in order to facilitate the microscopic analysis of the crystal structure.

### 2.3. Physical and mechanical tests performed on ITQ4

Physical and mechanical tests were carried out on the specimens both in natural condition and after ten years of natural weathering. The

description of the test is provided in the following.

Water absorption by immersion in water at atmospheric pressure (WA) was carried out according to EN 13755 (2008). WA is expressed as the percentage of water mass inside the pores of the specimen after 48 hours of saturation. Open Porosity test was performed according to EN1936 (2006) and the value represents the percentage of open voids connected to the surfaces of the specimen. According to previous scientific studies (Manfredotti and Marini, 2006, Vandevorde *et al.*, 2009), these methods are able to detect the weathering of a natural stone by comparing the results obtained on a fresh and weathered material.

Flexural strength was carried out to determine the resistance to flexural strength described by the European standard EN 12372 (2007). This test is a destructive method used to study the decay of stone and it is well correlated with non-destructive tests such as UPV and water absorption. The test has been performed on 200 x 50 x 30 mm specimens obtained from each slab.

Ultrasonic Pulse Velocity (UPV) is a very fast and efficient non-destructive methodology used to define the mechanical properties of a stone material. The test was carried out following the standard EN 14579 (2005). For each slab the indirect method has been applied using 250 kHz transducers. UPV is linked to the physical and mechanical characteristics of the material in which it propagates,

such as in terms of crystal texture, porosity and cohesion. The results of the tests are summarized in Table 1.

### 2.4. Quantitative pore structure analysis

In order to provide a quantitative characterization of the weathering effect on marble pore structure, we apply a methodology based on a modified version of A\* path-finding algorithm. The approach allows the analysis of 2D binary images of marble thin sections at different degrees of alteration. The A\* algorithm is able to identify the paths representative of the pore structure and to estimate, along each path, the aperture of the channels. The workflow of the methodology can be summarized in three steps:

- Image acquisition and processing
- Path identification in pore structure
- Pore size analysis

The above steps are described in the following sections.

#### 2.4.1. Image acquisition and preprocessing

The images have been acquired using a Leica M420 microscope (40X magnification) in \*.Tiff format at 12 Mpixels. Digital processing is applied to the images in order to highlight and extrapolate the impregnated paths. The procedure first involves a preliminary tuning of some of the main image parameters such as intensity, gamma, saturation, brightness and contrast. Secondly, a histogram-threshold-based mask is applied on the RGB values of the pixel image. The identified threshold is used to identify the impregnated domain and for the construction of a binary image in which the grain pixels are represented by the

Tab. 1 – Physical-mechanical test performed on the ITQ4 in natural condition and after ten years of natural weathering.

Performed tests	Not weathered slab	Naturally weathered slab
UPV f = 250kHz [m/s]	2725 ± 74	2205 ± 193
Open Porosity (%)	0,61 ± 0,04	1,65 ± 0,07
Water absorption WA [%]	0,20 ± 0,04	0,56 ± 0,05
Flexural strength [Mpa]	12,9 ± 3,5	9,2 ± 1,9

digital number 1 while the impregnated pore pixels by 0.

### 2.4.2. Path identification in pore structure

The pore structure of each generated image is characterized using a path-finding approach. Given a set of  $n_{in}$  inlets (start) and  $n_{out}$  outlets (target), automatically located along the boundaries faces of the porous domain (i.e. 2D image), the shortest paths between each inlet-outlet pairs is computed along the main considered directions (X, Y) (Viberti *et al.*, 2020) (Fig. 2).

A modified version of the A\* algorithm is used as a path-finding approach. The A\* approach (Hart *et al.*, 1968; Nilson, 2014) allows the construction of the optimal path (i.e. shortest) between two locations using an heuristic function to guide the search through the minimization of the cost function  $c_i(n)$ :

$$c_i(n) = g_i(n) + h_i(n) \quad (1)$$

where  $n$  indicates the considered node along the path,  $g_i(n)$  is the cost of the path from the start node (inlet) to a considered node  $n$  on the path,  $h_i(n)$  is the heuristic function representing a prior estimation of the cost to move from the considered node  $n$  to the target (outlet). The Euclidian distance is chosen as a forward cost  $h_i(n)$ . The path is constructed by progressively computing the cost function at each node from the inlet to the associated outlet. The final output is a graph  $G = (N, E)$  where  $N$  are a set of reference nodes progressively identified through the cost function with X - Y coordinates and  $E$  the connecting edges between nodes (2).

Since the marble could be poorly connected, the methodology was applied to image sub-windows. Moreover, a modified version of A\* was used in this work, which also allows the characterization of

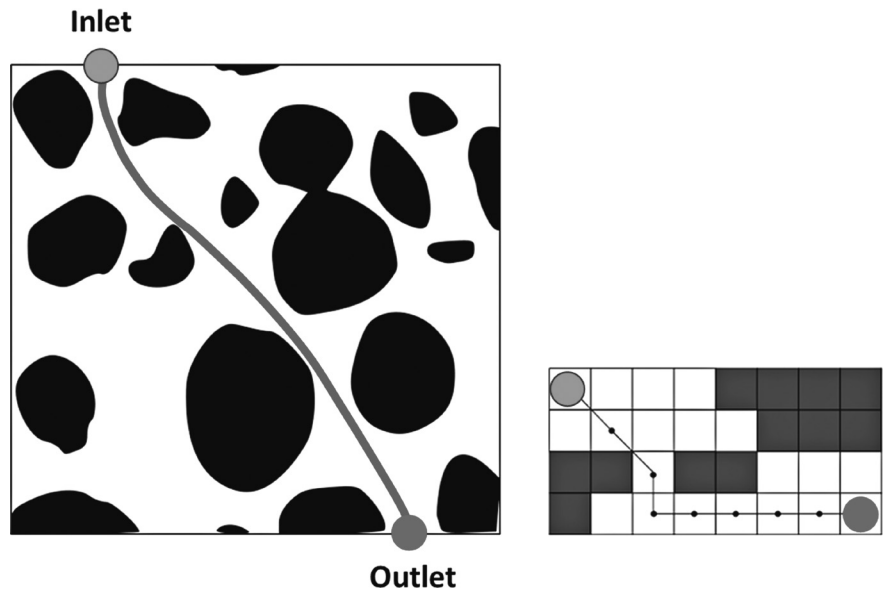


Fig. 2 – Schematic representation of an optimal path between an inlet/outlet pair:

dead-end paths (i.e. paths that are generated from a starting point that cannot reach the associated target because of obstacles).

### 2.4.3. Pore size analysis

The generated paths are used for the geometrical characterization of the pore structure. Along each identified geometrical path, the local pore size is estimated at each grid node location by measuring the extension of the pore section orthogonal to the local path direction (Fig. 3), therefore the total pore size distribution of the

porous domain within the image can be computed. The output provides a geometrical description of the pore size development along each simulated path and can be used for comparative quantitative analysis between pre and post rock weathering.

## 3. Results

Thin sections of marble samples described in paragraph 2, representative of pre and post weathering conditions, were analyzed and

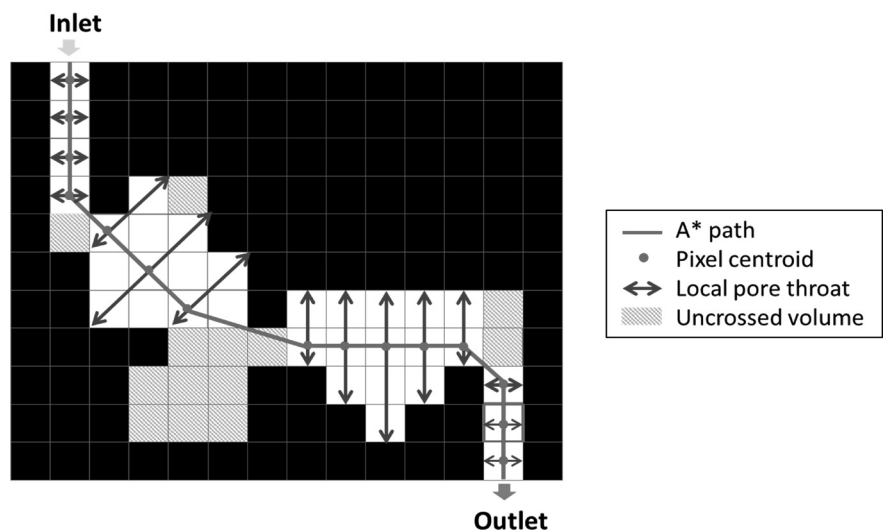


Fig. 3 – Qualitative representation of pore throat description along a path.

## AMBIENTE

compared. Two images of different subsections were considered in the non-weathered thin-section because of the presence of a significant variability within the sample.

Square subsection of 2.47 mm per side of impregnated pictures

are shown in Fig. 4 and the corresponding binarized images in Fig. 5. Each figure was divided into nine sub-windows of  $0.823 \times 0.823$  mm to increase the algorithm exploration in poorly connected areas. The path-finding based algorithm pre-

sented in section 3.2 was applied for each direction (N-S, S-N, E-W, W-E) in each of the nine sub-windows. The merge of all individual paths is shown in red in Fig. 6, where the sub-windows subdivision is displayed. For each path,

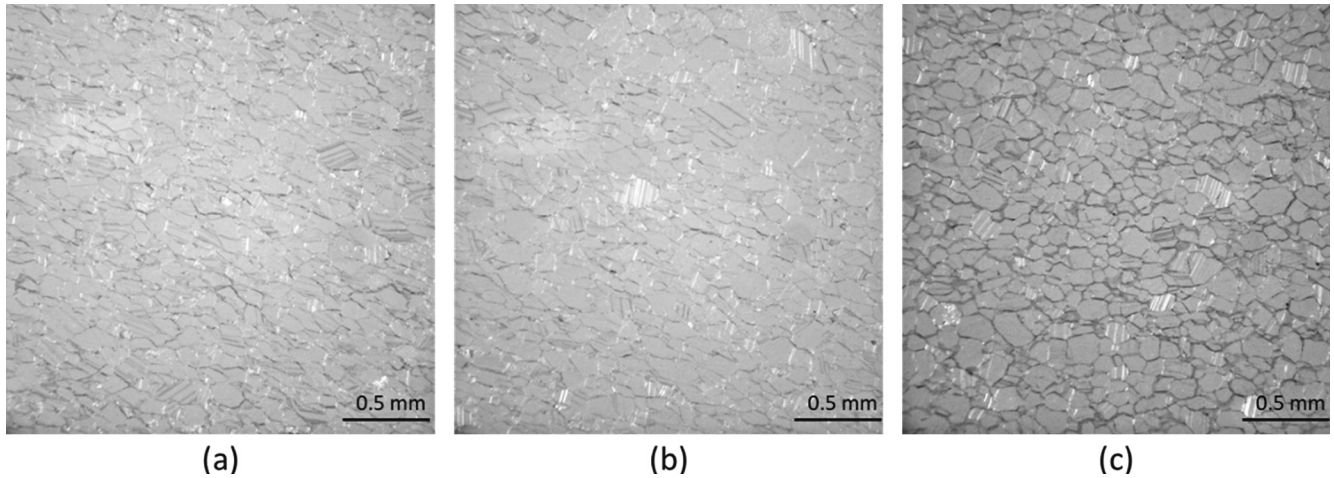


Fig. 4 – Thin sections of (a, b) non-weathered v.s. (c) natural weathering impregnated marble, after preliminary image processing. Figure resolution is  $0.8 \mu\text{m}$  per pixel.

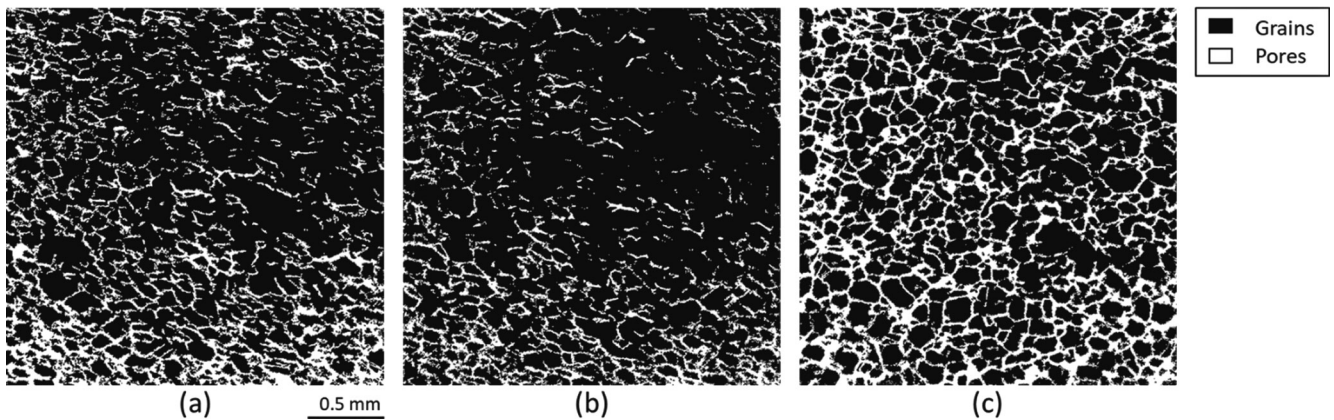


Fig. 5 – Binarized images of thin sections portions of (a, b) non-weathered and (c) natural weathering marble samples. Figure resolution is  $4 \mu\text{m}$  per pixel.

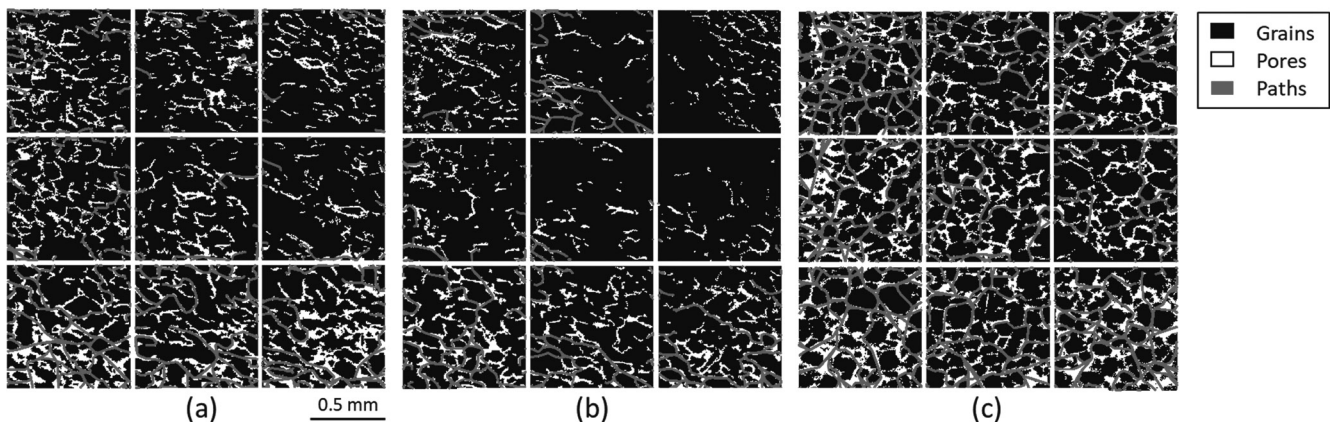


Fig. 6 – Paths individuated on the binarized pore structure images of Fig. 5, subdivided in 9 sub-windows of  $0.823 \times 0.823$  mm.

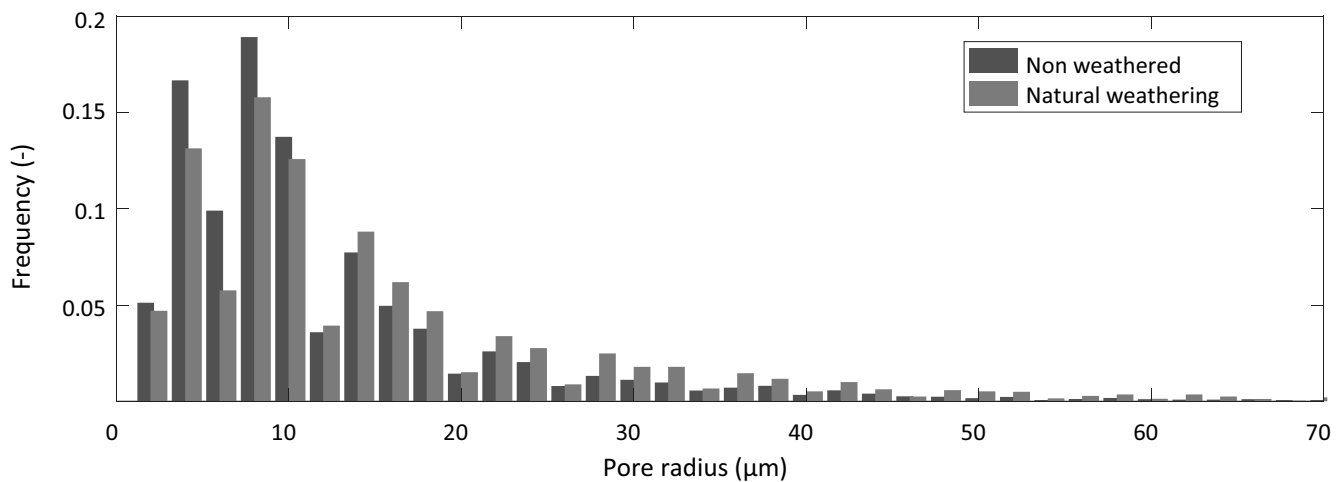


Fig. 7 – Comparison of pore radius distribution of non-weathered marble samples, in blue, and natural weathering, in orange.

the local pore radius was calculated as described in section 3.3. The resulting pore radius distributions before and after weathering are compared in Fig. 7. The comparisons between total porosity and quartiles of pore radius distribution is shown in Table 2.

#### 4. Discussion and conclusion

The presented work is an example of application of a methodology for pore structure analysis based on the A\* path-finding algorithm for characterizing ornamental stone degradation due to weathering.

Macroscopic images of impregnated thin sections representative of the Marble ITQ4, at natural conditions and after a long term natural weathering, were processed in order to obtain 2D binary images used as suitable inputs for A\* algorithm. Through the identification of the paths within the porous domain, the methodology allows the characterization of the pore structure in terms of pore radius distribution along the identified paths.

Results are summarized in Table 2 and Figure 7. The comparison between the considered param-

Tab. 2 – Porosity and pore radius distribution comparison between non-weathered and naturally weathered samples.

		Not weathered (a)	Not weathered (b)	Natural weathering (c)
Porosity (%)		18.3	11	28.5
Pore radius distribution	P25 (µm)	6	6	8
	P50 (µm)	10	8.4	11.3
	P75 (µm)	17	12	20

eters for the two non-weathered sections (a) and (b) indicate a degree of heterogeneity within the sample. However, the comparison between the porosity values and pore size distribution of the weathered (Fig. 4c) and the two non-weathered thin sections (Fig. 4a and 4b) clearly demonstrate a significant change in pore structure.

When comparing weathered with non-weathered thin sections (a) and (b), a significant increase in both porosity and pore size distribution is observed, especially with respect to the thin section (b), in which the third quartile (P75) of the pore radius distribution has almost doubled (from 12 µm to 20 µm) and the porosity has increased of a factor of 2.6 (from 11% to 28.5%). With regard to case (a), the increase of the third quartile (P75) of the pore radius distribution is limited to 17% (from 17 µm to 20 µm) and the porosity has increased of a factor of 1.5 (from 28.3 to 28.5).

The results obtained through image analysis highlight an incre-

ase in open porosity which occurred naturally in the specimen at 10 years exposure compared to the non-weathered sections, as reported in Table 1. The result is in good agreement with the experimental results demonstrating a decreasing of mechanical resistance measured by flexural strength and UPV (Tab. 1). In fact, the increase in the average size of the pores is closely correlated to the decrease in flexural strength, to the reduction in the ultrasound propagation speed and to an increase in open porosity.

Due to the high variability of the pore structure at the considered scale, analysis on a more extended number of thin sections is required to guarantee a statistical representativeness of the results.

#### References

Al-Raoush, R.I., Madhoun, I.T., 2017. TORT3D: A MATLAB code to compute geometric tortuosity

- from 3D images of unconsolidated porous media. *Powder technology*, 320, 99-107.
- Bellopede, R., Castelletto, E., Marini, P., 2016. Ten years of natural ageing of calcareous stones, *Engineering Geology*, vol. 211, Pages 19-26, ISSN 0013-7952, <https://doi.org/10.1016/j.enggeo.2016.06.015>
- Biscontin, G., Driussi, G., Maravelaki, P., Zendri, E., 1993. Physical-Chemical Investigations of Stone Architectonic Surfaces in Venice: The Scuola Grande Dei Carmini. in *Conservation of Architectural Surfaces: Stones and Wall Covering*, pp. 125-136.
- Biscontin, G., Graziano, L., 1993. Conservation of Architectural Surfaces: Stone Wall Covering, *Il Cardo*, Venice, pp. 125-136.
- Bortz, S., Stecich, J., Wonneberger, B., Chin, I., 1993. Accelerated weathering in building stone *Int. J. Rock Mech. Min. Sci. Geomech. Abstr.*, 30, pp. 1559-1562.
- Cai, J., Zhang, Z., Wei, W., Guo, D., Li, S., Zhao, P., 2019. The critical factors for permeability-formation factor relation in reservoir rocks: Pore-throat ratio, tortuosity and connectivity. *Energy*, Elsevier, vol. 188, 2019, 116051. ISSN 0360-5442. <https://doi.org/10.1016/j.energy.2019.116051>
- Camuffo, D., 1995. Physical weathering of stones *Sci. Total Environ.*, 167, pp. 1-14.
- EN 12372 Natural Stone Test Methods – Determination of Flexural Strength under Concentrated Load CEN Committee, Brussels, 2007.
- EN 13755 Natural Stone Test Methods – Determination of Water Absorption at Atmospheric Pressure CEN Committee, Brussels, 2008, p. 8.
- EN 14579 Natural Stone Test Methods – Determination of Sound Speed Propagation CEN Committee, Brussels, 2005, p. 12.
- EN 1936 Natural stone test methods. Determination of real density and apparent density, and of total and open porosity, 2006.
- Ghanbarian, B., Hunt, A.G., Ewing, R.P., & Sahimi, M., 2013. Tortuosity in porous media: a critical review. *Soil science society of America journal*, 77(5), 1461-1477.
- Hudec, P.P., 1998. Rock properties and physical processes of rapid weathering and deterioration. *Proceedings of the 8th International IAEG Congress, (IAEGC'98)*, Balkema, Rotterdam, pp. 335-341.
- Lindquist, W.B., Lee, S.M., Coker, D.A., Jones, K.W., & Spanne, P., 1996. Medial axis analysis of void structure in threedimensional tomographic images of porous media. *Journal of Geophysical Research: Solid Earth*, 101(B4), 8297-8310.
- Liu, J., Pereira, G.G., Regenauer-Lieb, K., 2014. From characterisation of pore-structures to simulations of pore-scale fluid flow and the upscaling of permeability using microtomography: A case study of heterogeneous carbonates, *Journal of Geochemical Exploration*, vol. 144, Part A, 2014, Pages 84-96, <https://doi.org/10.1016/j.gexplo.2014.01.021>.
- Manfredotti, M., Marini, P., 2006. The "Contact Sponge": Study of the Applicability of a New and Simple Methodology R. Fort, M.Á. de Buergo (Eds.), *Book of Abstracts of Heritage, Weathering and Conservation 2006*, Eighth Thematic Network on Cultural and Historic Heritage Scientific Meeting, Madrid (June 21-24, 2006).
- Molina Ballesteros, E., Cantano Martín, M., García Talegón, J. 2010. Role of porosity in rock weathering processes: a theoretical approach. *CADERNOS Lab. Xeolóxico Laxe Coruña* 35, 147-162.
- Øren, P.E., Bakke, S., 2003. Reconstruction of Berea Sandstone and Pore-Scale Modeling of Wettability Effects, *Journal of Petroleum Science and Engineering*, 39, 177-199.
- Rabbani, A., Jamshid S.i, Salehi, S., 2014. An automated simple algorithm for realistic pore network extraction from micro-tomography images, *Journal of Petroleum Science and Engineering*, vol. 123, Pages 164-171, Elsevier. doi: <https://doi.org/10.1016/j.petrol.2014.08.020>.
- Sassoni, E. & Franzoni, E. 2014. Sugaring marble in the Monumental Cemetery in Bologna (Italy): characterization of naturally and artificially weathered samples and first results of consolidation by hydroxyapatite. *Appl. Phys. A* 117:1893-1906.
- Sheppard, A.P., Sok, R.M., Averdunk, H., 2004. Techniques for image enhancement and segmentation of tomographic images of porous materials. *Phys. A Stat. Mech. Appl.* 339(1), 145-151.
- Siegesmund, S., Mosch, S., Scheffzük, Ch., Nikolayev, D.I. 2008. The bowing potential of granitic rocks: rock fabrics, thermal properties and residual strain. *Environ. Geol.* 55, 743-795.
- Siegesmund, S., Ullemeyer, K., Weiss, T., Tschegg, E.K. 2000. Physical weathering of marbles caused by anisotropic thermal expansion. *Int. J. Earth Sci.* 89, 170-182.
- Sing, K.S.W., 2004. Characterization of porous materials: past, present and future, *Colloids and Surfaces A: Physicochemical and Engineering Aspects*, vol. 241, Issues 1-3, Pages 3-7, (2004) ISSN 0927-7757, <https://doi.org/10.1016/j.colsurfa.2004.04.003>.
- Sun, W.C., Andrade, J.E., & Rudnicki, J.W., 2011. Multiscale method for characterization of porous microstructures and their impact on macroscopic effective permeability. *International Journal for Numerical Methods in Engineering*, 88(12), 1260-1279.
- Vandevorde, D., Pamplona, M., Schalm, O., Vanhellemont, Y., Cnudde, V., Verhaeven, E., 2009. Contact sponge method: performance of a promising tool for measuring the initial water absorption *J. Cult. Herit.*, 10.1, pp. 41-47, 10.1016/j.culher.2008.10.002.
- Viberti, D., Peter, C., Borello, E.S., & Panini, F., 2020. Pore structure characterization through path-finding and Lattice Boltzmann simulation. *Advances in Water Resources*, 103609.
- Warke, P.A., McKinley, J., Smith, B.J.,

2006. Weathering of Building Stone: Approaches to Assessment, Prediction and Modelling S.K. Kourkoulis (Ed.), *Fract. Fail. Nat. Build. Stones*, Springer, The Netherlands, pp. 313-327.
- Winkler, E.M., 1987. Weathering and weathering rates of natural stone *Environ. Geol. Water Sci.*, 9, pp. 85-92.
- Xiao, B., Wang, W., Zhang, X., Long, G., Fan, J., Chen, H., Deng, L., 2019. A novel fractal solution for permeability and Kozeny-Carman constant of fibrous porous media made up of solid particles and porous fibers, *Powder Technology*, vol. 349, 2019, Pages 92-98, ISSN 0032-5910, <https://doi.org/10.1016/j.powtec.2019.03.028>.
- Xu, P., Yu, B., 2008. Developing a new form of permeability and Kozeny-Carman constant for homogeneous porous media by means of fractal geometry, *Advances in Water Resources*, 31(1), pp. 74-81, ISSN 0309-1708, <https://doi.org/10.1016/j.advwatres.2007.06.003>.
- Yao, J., Hu, R., Wang, C., Yang, Y., 2015. Multiscale Pore Structure Analysis In Carbonate Rocks, *Journal for Multiscale Computational Engineering*, 13 (1): 1-9.